International Journal of Technology 14(4) 932-947 (2023)
Received October 2021 / Revised January 2022 / Accepted January 2023

International Journal of Technology

http://ijtech.eng.ui.ac.id

High Throughput and Low Latency Wireless Communication System using Bandwidth-Efficient Transmission for Medical Internet of Thing

Astri Maria Kurniawati[1*], Nana Sutisna[1], Hasballah Zakaria[1], Yuhei Nagao[2], Tati L. Mengko[1], Hiroshi Ochi[2]

[1]*School of Electrical Engineering and Informatics, Institut Teknologi Bandung, Jl. Ganesha 10 Bandung 40132, Indonesia*
[2]*Department of Computer Science and Electronics, Kyushu Institute of Technology, Kawazu 680-4, Iizuka, Fukuoka 820-8502, Japan*

Abstract. This paper presents a high throughput and low latency wireless with efficient bandwidth transmission, particularly for Medical Internet of Things (MIoT) applications. The proposed method is obtained by employing shorter OFDM (Orthogonal Frequency Divison Multiplexing) symbol duration which corresponds to shorter packet transmission. This can be realized by reducing subcarrier spacing and allowing to use of a smaller number of sample data in the time domain while maintaining sampling rate frequency. Furthermore, the proposed scheme can transmit more data frames twice within the original time slot duration, hence, it can enhance the throughput without expanding the bandwidth utilization. The evaluation results of 20 MHz and 40 MHz bandwidth cases show throughput improvement by around 2.3 and 2.6 times compared to the conventional ones. In addition, the proposed scheme also provides low latency transmission by reducing the transmission time by around 50%. The corresponding hardware implementation is also provided with low-complexity hardware resources. Hence, the proposed system can be used for IoT systems with main considerations on low latency, high throughput, bandwidth efficiency, and low power consumption.

Keywords: High throughput; Low latency; Medical IoT; Smart healthcare; Wireless communication

1. Introduction

Recently, during global pandemic situations, the role of a smart healthcare system has become more important since it can reduce physical contact. This can be realized by leveraging the Medical Internet of Things (MIoT), where the diagnosis, patient monitoring, consultation, or accessing health records can be carried out remotely (Janjua, Duranay, and Arslan, 2020). The MIoT system is not only deployed for real-time monitoring of various sensors that provide medical data of patients but also can be used for a wide range of applications, including teleconsultation services that deliver high-resolution images or videos. These services require high throughput and huge bandwidth transmission (Ahmed *et al.,* 2020; Ahad *et al.,* 2020; Marques *et al.,* 2019; Alam *et al.,* 2018). In addition, the MIoT also incorporates various data sizes collected from many medical instruments (Jagadeeswari *et al.,* 2018). Other performance metrics that should be considered in the related medical system are security and reliability issues (Ali *et al.,* 2018).

*Corresponding author's email: maria.astri@office.itb.ac.id, Tel.: + 62 22 2534117; Fax: + 62 22 2534117
doi: 10.14716/ijtech.v14i4.5234

The MIoT system is also expected to support fast response systems such as in telesurgery and telemonitoring applications, especially for patients who have high risk. This application requires a low latency communication (e.g. end-to-end time to deliver packet data from source to destination) to guarantee the data is successfully transmitted, for example requiring transmission in millisecond order. These requirements impose an IoT device to achieve higher performance requirements, specifically minimum latency and higher network bandwidth, to satisfy end-to-end system performance (Ahmed *et al.,* 2020; Ahad *et al.,* 2020; Shukla *et al.,* 2019; Alam *et al.,* 2018). Different applications of medical IoT require various latency and bandwidth. For example, in real monitoring of patient health data and vital sign measurements, the latency could be around 10 ms up to 700 ms, and in a teleconsultation case, it can be around several hundreds of milliseconds. Meanwhile, for telesurgery and emergency communications (fast alert or quick reply), the latency requirement is less than 100 ms (Skorin-Kapov and Matijasevic, 2010). To obtain low latency transmission, several methods have been proposed on both the upper layer and low layer (physical layer/ PHY). In the upper layer, Low Latency Queuing Algorithm that developed proper scheduling for different QoS is proposed (Rukmani and Ganesan, 2016). Another method to obtain latency communication is by reducing the small number of retransmissions, which corresponds to providing reliable packet transmission. In this case, a redundant-based transmission can be employed as proposed by Ng *et al.* (2019).

Wireless communications are essential for future smart healthcare since it has flexible and scalable connectivity. Several communication technologies have been considered for healthcare IoT, which are Bluetooth, ZigBee, Wi-Fi, and cellular systems (WiMAX and LTE). WLAN (Wireless Local Area Network) technology is a potential solution for achieving high throughput transmission. Recently, WLAN has gained popularity to be used as a communication interface in IoT devices, including MIoT systems due to simple setup/installation, high interoperability, and low cost of deployment. The existing WLAN technology is potentially deployed for a healthcare system, however, for time-constrained applications, it requires some improvements.

The previous WLAN communication protocol has several limitations, particularly for applications that require low latency and efficient bandwidth transmission. First, the WLAN packet structure (frame format) is essentially designed for generic data communication, such as voice and video transmission, which is not targeted for transmitting short packets. Hence, it results in an inefficient transmission from the point of view of transmission latency. Moreover, to transmit high data volume for high throughput, the general WLAN protocol requires higher bandwidth, such as 40 MHz or 80 MHz. The bandwidth resource becomes limited due to the rapid growth of the number of deployed devices. This existing large number of devices in the same network can raise interference and the difficulty of network planning which leads to poor performance efficiency (Adelabu, Imoize, and Ughegbe, 2021). Hence, bandwidth utilization becomes challenging and should be managed.

Short packet transmission has been investigated as a new research direction, particularly to be employed in a wireless system that involves data generated by sensors and other machine-to-machine (M2M) communications (Durisi, Koch, and Popovski, 2016). Several methods have been proposed dealing with short packet communications in different layers, physical and mac layer (upper layer). Luvisotto *et al.* (2017) proposed a customized frame structure to obtain short packet transmission by utilizing a short preamble and a reduced length of cycle prefix. Hence, the total data overhead can be reduced. However, this modification requires modification in the overall system protocol since it does not comply with the standard and thus the system must be deployed in a

dedicated network. As a result, it cannot use the existing wireless protocol. Other methods to achieve short transmission are considering new waveforms, such as filtered Cyclic Prefix Orthogonal Frequency Division Multiplexing (CP-OFDM) and Filter Bank Multicarrier (FBMC) (Schaich, Wild, and Chen, 2014). These techniques enable fast time interval switching between downlink and uplink transmission. However, in terms of complexity, those implementations require a high-complexity receiver. Therefore, it is not suitable for low-power systems such as IoT.

To overcome those limitations, in this paper, we propose a method to achieve low latency communication while offering efficient bandwidth transmission with low complexity implementation. First, to achieve low latency communication we reduce packet transmission time. The WLAN packet is shortened by reducing sub-carrier spacing in each OFDM (Orthogonal Frequency Division Multiplexing) symbol. This method offers two main advantages at the same time. First, it does not modify packet structure and thus the overall signal processing remains similar and we may use the previous conventional WLAN system. The second one, the longer packet payload can be sent in a similar time compared to a conventional method. Hence, the wider bandwidth or multi streams/antenna transmission (MIMO – Multiple Input Multiple Output technique) can be avoided. In this case, the efficient bandwidth is utilized with low complexity. Moreover, in terms of power consumption metric, the proposed method will also offer low power consumption (i.e., energy efficient) systems. In summary, the proposed work is suitable for IoT systems, where the performances of low power consumption, small bandwidth, and low complexity are the main consideration.

However, it should be noticed that the use of smaller subcarrier spacing would result in either large EVM (Error Vector Magnitude) due to phase noise or more stringent requirements on the local oscillator. Moreover, the small subcarrier spacing further leads to performance degradation in mobility scenarios due to high doppler effects. Hence, the design of receiver parts, for example, timing synchronization, channel estimation, and demodulation should be carried out carefully to mitigate these issues unless the proposed system will have poor performance in terms of a higher error rate.

The main contributions of this work are summarized as follows:

a) We shorten the packet transmissions by reducing the period of OFDM symbols, Specifically, by reducing sub-carrier spacing.
b) We employ cross-layer design to perform optimization and evaluate the impact of the employed system parameters on the performance metrics. From this step, we can obtain optimum system parameters that offer balanced performance between transmission time, reliability, and system complexity.
c) We present a corresponding hardware design, implementation, and performance evaluation.

The rest of this paper is structured as follows. Section 2 describes the details of the proposed system, including the system model, proposed transmission scheme, and corresponding hardware architecture design. In section 3, we discuss performance results. Finally, section 4 presents the conclusion.

2. Proposed System

In this section, we will discuss the proposed PHY design systematically, incorporating system models, proposed transmission scheme, architecture design as well as design optimization.

2.1. System Model

First, to simplify the baseband PHY transceiver we consider a baseline (conventional) OFDM system as shown in Figure 1.

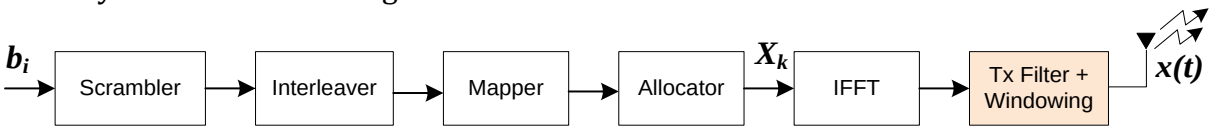

Figure 1 OFDM baseband transmitter model

The binary data, b_i firstly are taken from the payload data source and then proceeded by scrambler and interleaver. Subsequently, the bits are mapped according to the employed modulation scheme by a mapper block. After mapping data into a group of symbol data (e.g. sub-carrier), the reference pilot data are inserted. These reference data pilots are mainly used for channel estimation in the receiver. The data subcarriers and pilot subcarriers are assigned to the appropriate index position of an OFDM symbol, X_i.

An OFDM baseband symbol is provided by modulation of N complex data, by employing Inverse-Fast-Fourier-Transform (IFFT) block. To avoid inter-symbol interference (ISI), a guard interval (GI) is appended to each symbol. Therefore, the OFDM symbol becomes $N + N_g$ samples in total. The transmitted symbol is given by Equation (1):

$$x^i(t) = x^i_{n,l} = \frac{1}{N}\sum_{k=-\frac{N}{2}+1}^{k=\frac{N}{2}} X^i_{k,l} e^{\frac{j2\pi kn}{N}}, \;\; n = -N_g, \dots, N-1 \tag{1}$$

where $x^i(t)$, $x^i_{n,l}$, and $X^i_{n,l}$ represent the transmit signal in a continuous time-domain, n^{th} discrete time-domain, k^{th} complex frequency-domain from l^{th} symbol and i^{th} transmit antenna respectively. Furthermore, the continuous transmit signal passes through the digital-to-analog converter (DAC) before being transmitted over a wireless channel.

At the receiver module, the time-domain signal, $y(t)$ is obtained by convolving the transmit signal $x^i(t)$ and the channel impulse response $h^i(t)$ and also adding the additive white Gaussian noise (AWGN), $w(t)$as expressed in Equation (2).

$$y(t) = x(t) * h(t) + w(t), \tag{2}$$

where $(*)$ is a convolution operator. For simplification, we omit the notation of i.

After removing the GI part, the FFT block transforms N discrete continuous samples into frequency-domain and results in the received signal $Y_{k,l}$. Finally, the estimated transmitted signal can be obtained through an equalizer (e.g. MIMO decoder for a multi-antenna system):

$$\widehat{X_k} = H_k^H\left[\sigma^2 I + H_k H_k^H\right]^{-1} Y_k \tag{3}$$

here, σ^2 denotes the noise power, $(.)^H$ and I represents the Hermitian transpose and the identity matrix, respectively. The latter, the estimated received signal will be preceded by the rest blocks of the receiver system, resulting in the received payload bits, in terms of PSDU data (e.g. RX PSDU).

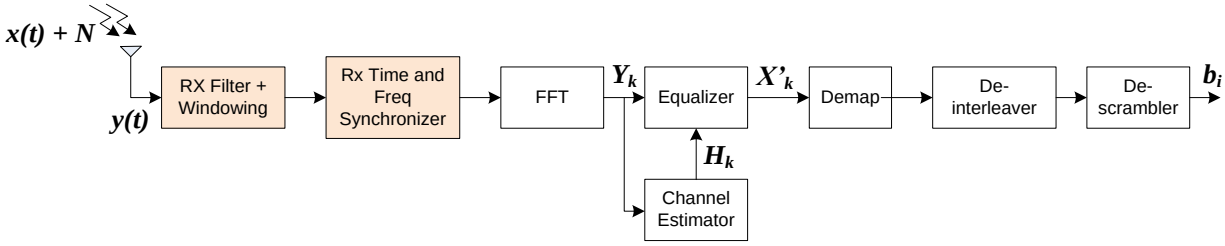

Figure 2 OFDM baseband receiver model

From this basic structure of the transceiver system, we identified that the relevant modules to be modified for achieving shorter transmission are the time-dependent modules that perform data processing in the time domain. These blocks include TX/RX Front end such as filter, windowing, and sampling unit (shown as highlighted block diagrams). In addition, the main control is also required to adjust the timing requirements.

2.2. Packet Format and OFDM timing parameters

In this section, we provide a brief overview of the packet structure of the WLAN system to give a better understanding of system parameters. This will be fundamental when we need to modify the transceiver system for achieving low-latency transmission. The recent WLAN standard uses OFDM-based transmission at the PHY layer and performs transmission on a frame/packet basis. To allow frame detection, the preamble part is appended to data payload from the upper layer (e.g. MAC Service Data Unit - MSDU) and construct PLCP Packet Data Unit (PPDU). The preamble length varies according to the employed packet format as given by:

$$T_{pre} = \begin{cases} 5T_{sym}, & for\ Legacy\ Format\ (802.11a/g) \\ 7T_{sym}, & for\ HT\ Format\ (802.11n) \\ 10T_{sym}, & for\ VHT\ Format\ (802.11ac) \end{cases} \quad (4)$$

where T_{sym} denotes the duration of one OFDM symbol.

Furthermore, the overall packet transmission time, T_{packet} for a PPDU packet can be expressed as:

$$T_{packet} = T_{pre} + T_{sym}N_{data\_sym}\ , \quad (5)$$

where, N_{data_sym} is the length of the payload date in terms of the OFDM symbol unit. The number of OFDM symbols contained in the data payload can be calculated as follows:

$$N_{data\_sym} = \left\lceil \frac{L}{N_{dsc}N_{ss}Rlog_2(M)} \right\rceil \quad (6)$$

Equation (4) implies that the packet length is affected by system parameters that correspond to latency and throughput performance, which are coding rate (R), modulation order (M), several spatial streams N_{ss}. The parameter N_{dsc} denotes the number of data subcarriers, where the number varies depending on the employed frame format.

In this work, the system-level design aims to find the optimal OFDM parameters that can minimize the total packet transmission time as directed by the upper layer protocol. Some parameters have been fixed due to the following reasons: (1) the limitation of hardware capabilities, (2) consideration of low-complexity implementation, or (3) low power consumption. The fixed parameters have been determined, which are the number of spatial streams, N_{ss}, that corresponds to the number of transmit antennas or the payload size, L, which has been specified from the upper layer as it is application dependent. Specifically, we employ one spatial stream (1 transmit and receive antenna) and a maximum payload size of 200 bytes.

2.3. Proposed Bandwidth-Efficient Transmission Scheme

The conventional WLAN-based system transmits payload data in packet-based transmission, where each packet consists of several OFDM symbols. As defined in the WLAN standard (IEEE, 2013) one OFDM symbol has a fixed time duration which is 3.2 μs. In one OFDM symbol, a set of subcarriers are utilized, depending on the employed transmission bandwidth.

Since the transceiver usually is designed to support multi-mode of transmission bandwidth, the data to be OFDM-modulated in FFT are constructed with different numbers of sub-carriers and further oversampled accordingly, using similar system clock frequency. For example, in 20 MHz bandwidth transmission, 64 sub-carrier data are modulated and applied to 4 times oversampling at 80 MHz clock, forming 256 data samples in the time-domain and it is equivalent to 3.2 μs transmit signal. This conventional transmission scheme is depicted in Figure 3.

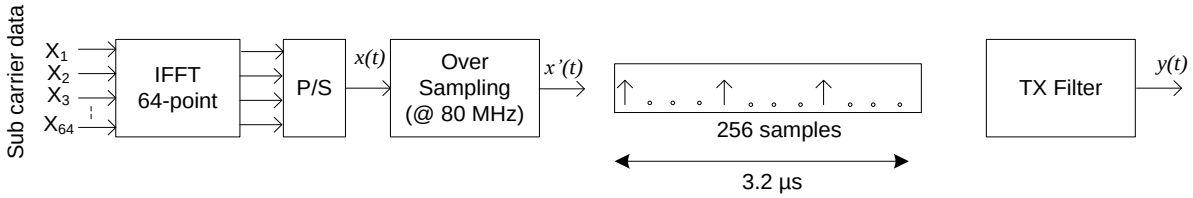

Figure 3 Conventional Transmission Scheme (20 MHz)

To transmit data in higher throughput, the data could be transmitted using higher bandwidth transmission, for example using 40 MHz of bandwidth. Unfortunately, the higher transmission mode is not feasible in low-complexity devices such as in IoT systems, due to cost and power limitations. Hence, to achieve the same throughput and latency performance as in higher bandwidth, the transmission scheme is modified. The idea is to reduce the OFDM symbol duration by around half of the conventional scheme. To realize this objective without modification of any signal processing (i.e. keep the number of data the same), the spacing between sub-carrier data is reduced to 156.25 KHz. Hence, for 20 MHz bandwidth with 64 sub-carriers, the 64-point FFT can still be used to perform OFDM modulation for each OFDM symbol. This is equivalent to an OFDM symbol length of 1.6 μs. As a result, within 3.2 μs we can double the capacity of transmission to become two OFDM symbols, as illustrated in Figure 4.

In addition, since we use the same FFT design (same FFT point) and sampling rate clock (system clock), we can also reduce the sampling rate (the number of inserted zero samples) to become only one data between 2 samples, removing two zero data as in conventional. Therefore, for the same time slot, we can transmit the data payload twice. This is similar to when we perform transmission with higher channel bandwidth. However, in our approach, the actual transmit bandwidth is still 20 MHz, which makes the channel utilization efficient.

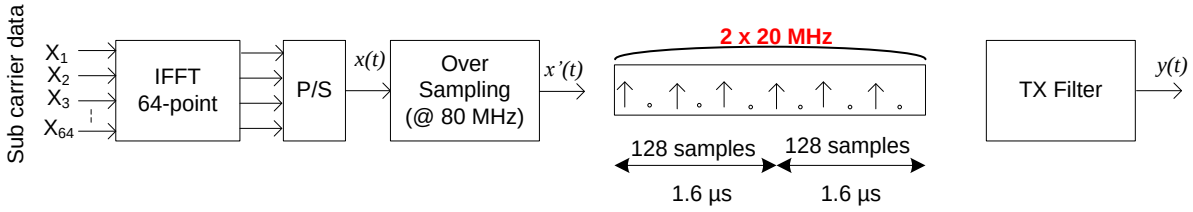

Figure 4 Proposed Transmission Scheme (20 MHz)

To be clear, we formulate this scheme as follows. Let, the payload length of data to be transmitted are *L* bits and the usable bandwidth is *W*. Assume, the time to transmit data using the original scheme is *T*, where the *T* follows T_{packet}, as described in Equation (5). By reducing the oversampling ratio after the IFFT process from 4 to 2 and preserving the system clock at 80 MHz, the length of each OFDM symbol becomes $\frac{T_{sym}}{2}$. Therefore, the total frame length of each transmitted packet will be $\frac{T_{packet}}{2}$. As a result, within the same transmission interval, *T*, now we can transmit two packets using the same transmission

bandwidth, increasing the system throughput. In the point of transmission, the proposed system can achieve low latency transmission even using lower bandwidth. Therefore, we can use available bandwidth efficiently.

In addition, by reducing the number of sample rates, the design of front-end modules, such as TX/RX filter and synchronization also becomes less complex and results in smaller hardware resources in hardware implementation. This issue will be explained in a later section.

2.4. PHY Architecture Design

In this section, we will discuss the corresponding PHY hardware architecture of the proposed transmission scheme.

2.4.1 Overall PHY Block Diagram

The original design of the PHY transmitter and receiver system that supports 20/40 MHz bandwidth corresponds to Figure 5 and Figure 6, respectively.

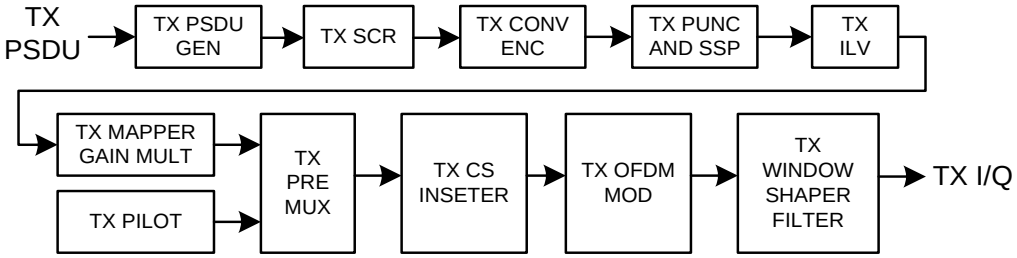

Figure 5 Transmitter Architecture block diagram

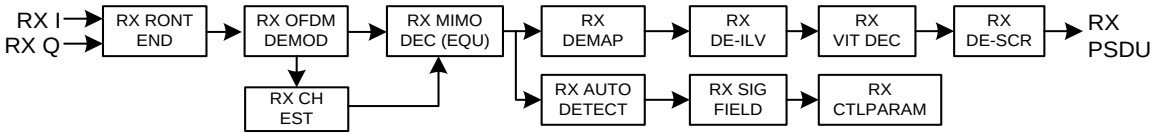

Figure 6 Receiver Architecture block diagram

To obtain a data frame (packet), the transmitter performs several processes sequentially, involving a scrambler, convolutional encoder, and interleaver block before proceeding into individual antenna paths (stream). The input payload data for the PHY transmitter is provided by the upper layer in a shared memory block. The transmitter also received parameter settings, which is TXVECTOR from the upper layer. Later, the TX data goes through the following modules which are Mapper, Pilot Inserter, IFFT, and GI (Guard Interval) Inserter. The final processing in the transmitter is time domain processing, which is Windowing and TX Filters that perform waveform shaping and fine-tune transmission data rate.

The receiver, as shown in Figure 5, mainly consists of two main processes, which are the time-domain processing in the front-end unit and frequency-domain processing. The receiver front-end performs several functions related to initial frame reception (synchronization), Gain adjustments (Automatic Gain Controller), and estimation/compensation of phase, frequency, and sampling error. The frequency domain processing involves several modules for example Channel Estimator, Phase Tracking, and MIMO Decoding to recover the impairments of the received signal due to channel effect. First, the Channel Estimator will estimate the channel characteristics which are channel response. Then, the calculated channel response will be used to equalize the received data performed by the MIMO decoder. Furthermore, the decoded data will go through the following blocks which are de-interleaver, Viterbi decoder, and descrambler. The final

received data bits (RX PSDU) are formed as packet payload and sent to RX MAC. To summarize, Table 1 provides several important PHY parameters.

2.4.2 Design Modification

To accommodate the proposed scheme, some modifications are required, in particular for bandwidth-related processing. In the transmitter system, several blocks proceed data according to employed bandwidth such as the IFFT module that performs OFDM modulation and TX Filter for windowing and shaping the waveform. The modifications are explained below.

Table 1 System parameters of PHY design

Parameters	Conventional PHY System	Proposed PHY System
Number of Antenna	1-4	1
Frame Type	Legacy, Mixed HT, Mixed VHT	Legacy, Mixed VHT
Channel BW	20/40 MHz	20 MHz
FFT Size	64/128 point	64 point
Symbol duration	3.2 μs	1.6 μs
Subcarrier Spacing	312.5 KHz	156.25 KHz
GI Duration	0.4/0.8 μs	0.4 μs
Sampling Freq.	80 MHz	80 MHz
Oversampling Ratio	2/4	2
Forward Error Correction (FEC) Scheme	Convolutional Code	Convolutional Code
Modulation Coding Scheme (MCS)	BPSK, QPSK, 16-QAM, 64-QAM	BPSK, QPSK, 16-QAM, 64 QAM

a) 64-point IFFT/FFT

The original PHY design uses configurable IFFT which supports 20 and 40 MHz transmission by employing 128-point IFFT. The FFT computation is considered a high computation module in the transmitter, that affects system complexity and timing processing. Hence, reducing the size of the FFT point will significantly reduce the hardware complexity.

Since the proposed transmission scheme is only targeted to employ a single bandwidth of 20 MHz, the 64-point IFFT/FFT is sufficient for modulating data in OFDM transmission. The FFT/IFFT module is designed using a radix-2 structure as a balanced trade-off between hardware complexity and achievable processing time. Practically, a reduction in the number of FFT points can significantly reduce the number of hardware resources, specifically, the number of multiplication and addition will be reduced by around 60 % (Azim, 2013). In addition, the processing latency of 64-point FFT is also reduced by around 50 %, from 137 clock cycles to 70 clock cycles, for processing each OFDM symbol.

b) Low-pass Filter

The digital filters in the transmitter front end are usually employed to perform signal waveform shaping with the intended bandwidth as well as remove signals outside the occupied bandwidth. To achieve good performance, there are some requirements for the spectrum of the yhr transmitted signal as defined by the spectral mask. A transmit spectrum mask specifies the power contained in a specified frequency bandwidth, and the amount of allowed power that can be emitted from a transmitter at the center frequency and at given frequency points, which is usually have been regulated by an authorized institution. As we can see from the IEEE 802.11 standard, the minimum rejection of spectral mask is around 20 dB. To achieve this requirement, the employed filter in the front-end part should be capable of rejecting unwanted signals at least 20 dB. Hence, this parameter is considered a minimum specification of a digital filter.

Furthermore, from the perspective implementation, for a fixed nominal bandwidth and predefined minimum sideband rejection, the performance of digital is affected by filter order (i.e. number of filter coefficients) which is proportional to the employed oversampling ratio. A higher filter order is required to achieve the same performance at a higher sampling rate.

In general, a low pass filter can be expressed as a convolution process between a set of constants, namely, filter coefficient h, and input signals x. The filter process can be expressed in the following equation (7):

$$y(n) = h(n) * x(n) = \sum_{k=0}^{L-1} h(k)x(n-k) \quad (7)$$

where L denotes the filter length or filter coefficient.

To achieve spectral mask requirements, the low pass filter in the conventional transmission scheme requires a 31-order filter (i.e. 31 filter coefficients). The implemented filter is characterized by the impulse response and frequency response, as depicted in Figure 7 and Figure 8, respectively. Furthermore, the impulse response obtained in Figure 7 will be used as a filter coefficient to perform filter calculation as shown in Figure 9. On the other hand, from Figure 8 we can see that the frequency response from the designed filter has met the requirement of a spectral mask, where the rejection sideband of the filter is around -20 dB. Therefore, we can validate that the designed filter satisfies the specification of a spectral mask.

From the implementation perspective, by directly implementing Equation (5), the implemented FIR requires 31 multipliers, 31 registers, and 30 adders, which can be realized by FIR architecture in Figure 9. However, by exploiting the symmetry of the designed filter coefficient, in which $h(k) = h(L-k)$, except for $k \neq \frac{L}{2}$ as the center point of the impulse response, we may rearrange the filter structure by using flipped architecture. Hence, the required multipliers could be reduced to 16. Furthermore, in practical implementation, since there are some small values of filter coefficients, toward zero, we also may omit this coefficient to reduce calculation. Hence, the required number of coefficients is 12 effectively, which is equivalent to 12 multipliers.

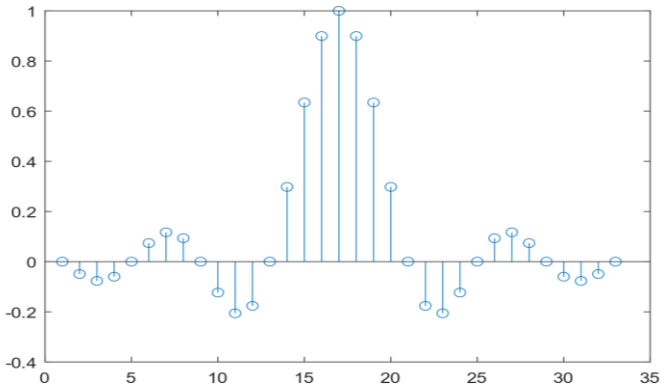

Figure 7 Filter Impulse Response (Filter Coefficients)

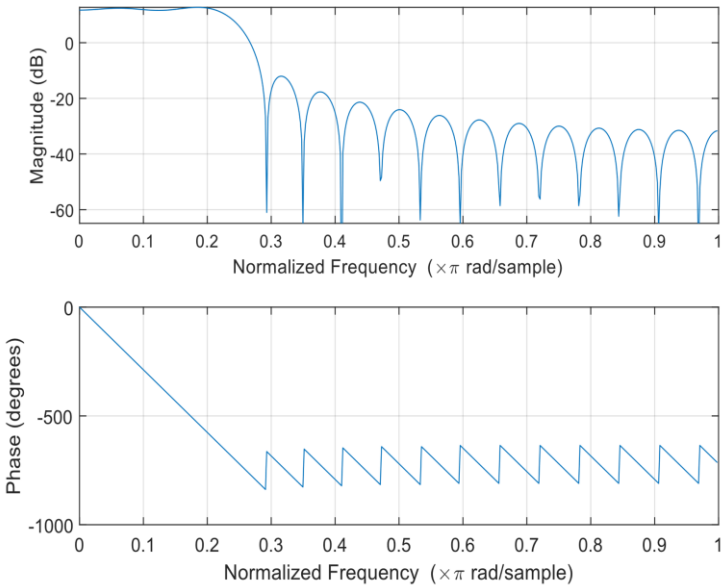

Figure 8 Frequency Response of the designed filter

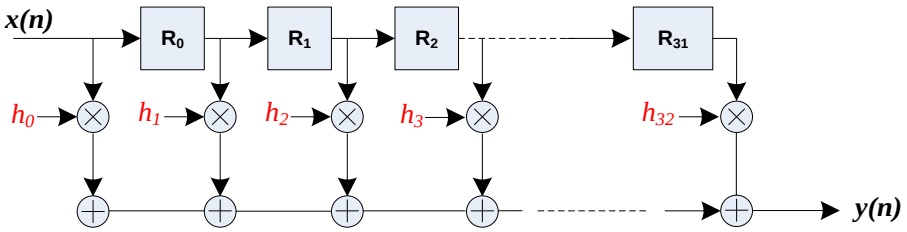

Figure 9 Direct implementation TX Filter

Using the same design approach, we also can derive the filter design for the proposed system. Since the proposed transmission scheme only employs two times oversampling, the required filter order becomes half of the conventional one, which is only 15. By employing a similar flipped structure, the effective multiplication will be 8. Furthermore, by also omitting some coefficients with near zero values, the final filter architecture only requires 4 multipliers, 8 adders, and 15 registers. This implies that the designed filter for the proposed system saves almost half the processing element, which is less complex than the conventional (original) system.

c) Receiver front-end

The receiver front-end has several tasks related to the acquisition of received signals, timing synchronization, and frequency offset compensation. These tasks perform their data processing according to the employed sampling rate as well as bandwidth.

- **RX filter** should be modified to accommodate oversampling ratio changes. The RX filter uses a similar design to the TX filter, as we have described in the previous discussion.
- **The synchronizer** module usually performs cross-correlation with the known pattern, which is preamble signals to determine the start of an incoming frame. In practice, to determine the correct incoming frame, a matching filter is employed.

Since the number of preamble patterns is shortened due to the reduction of the sampling rate, the filter match needs to be modified accordingly. Specifically, the preamble pattern for the matched filter needs to be reduced from 64 samples to 32 samples. However, since the preamble part is constructed from 4 repeated patterns, we may use the first 16 samples.

d) Control Circuits

The control unit also requires some modification, in particular for sample-dependent parameters, the limit (maximum counting) of a counter, as well as generation timing signals for latency adjustments.

3. Performance Results and Discussions

In this evaluation, each packet of data consists of 200 bytes, considering the packet length in medical IoT has a relatively short packet. In this evaluation, the total transmitted packets were 1000 frames. The simulation setup also takes into account various impairments, such as the nonlinearity of the Power Amplifier (PA), phase noise, Carrier Frequency Offset (CFO), and bit quantization model of ADC/DAC to reflect real-world conditions. Furthermore, the TGn Channel D (Erceg *et al.*, 2004) is considered a channel model to reflect typical indoor/office environments as a general use case of deployment of a MIoT system, where the transmitter-receiver is set by around 20 m.

3.1. System Error Rate Performance

Error performance evaluations are the critical performance metrics in a wireless system. It is not only affecting system reliability but also given an impact on the system latency. If the data transmission has a higher error rate, it will require additional packet retransmission to deliver data successfully, and this results in longer transmission latency as well as reduced transmission throughput. However, in the current system, we focus on the physical layer design. Hence, retransmission will not be implemented.

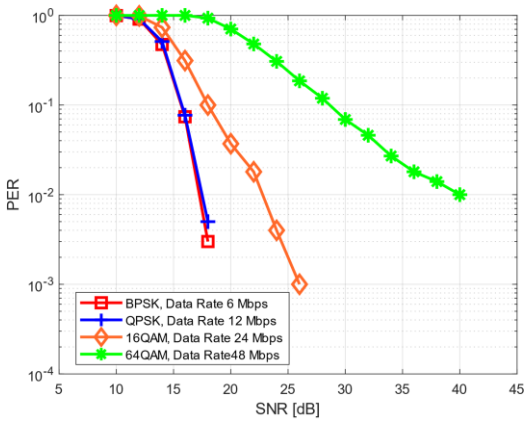

Figure 10 PER performance of Legacy Frame Format

Figure 10 shows examples of PER performance for various MCSs (Modulation Coding Schemes) settings. The simulation confirms that employing higher MCS will reduce system reliability. For example, at the same channel condition (i.e. similar SNR value), the MCS0 and MCS2 can achieve PER (Packet Error Rate) less than 1% for SNR lower than 16 dB. However, MCS4 and MCS6 require 22 dB and 40 dB of SNR to achieve a PER performance of around 1 %. This reveals that there is a trade-off between reliability, data rate, and transmit power, which needs to be considered carefully to deploy optimum systems.

3.2. Throughput Performance

Throughput performance is defined as the amount of payload data that is successfully delivered to the receiver within a certain total transmission time. Let's assume the L byte of payload could be transmitted within the interval time of T. If the payload data is sent repeatedly k times at the channel condition of packet error rate, α, the throughput, Γ can be calculated as:

$$\Gamma = \frac{(1-\alpha)kL}{kT} = \frac{(1-\alpha)L}{T} \quad (8)$$

Based on the obtained PER results in Figure 10, the throughput performance of the conventional system and the proposed system can be obtained, and it is shown in Figure 10. As shown in Figure 11(a), for the case of MCS0, which is BPSK modulation, the system can achieve up to 5 Mbps at good channel condition and offer the highest effective throughput 20 Mbps, when employing 64QAM modulation. On the other hand, by employing the proposed transmission scheme, we can improve the throughput up to two times the conventional scheme, as confirmed by evaluation results in Figure 11(b). The results in Figure 11 show that the effective throughput performance is lower than the maximum achievable data rate, as defined in the standard. This throughput performance degradation is caused by the overhead of preamble data. In a short payload transmission, the preamble data will take a significant portion of the overall packet length, specifically in the higher order MCS such as 16QAM and 64 QAM. The preamble portion could occupy almost 80% of the total packet length. Therefore, we need to consider the optimum payload to maximize achievable throughput.

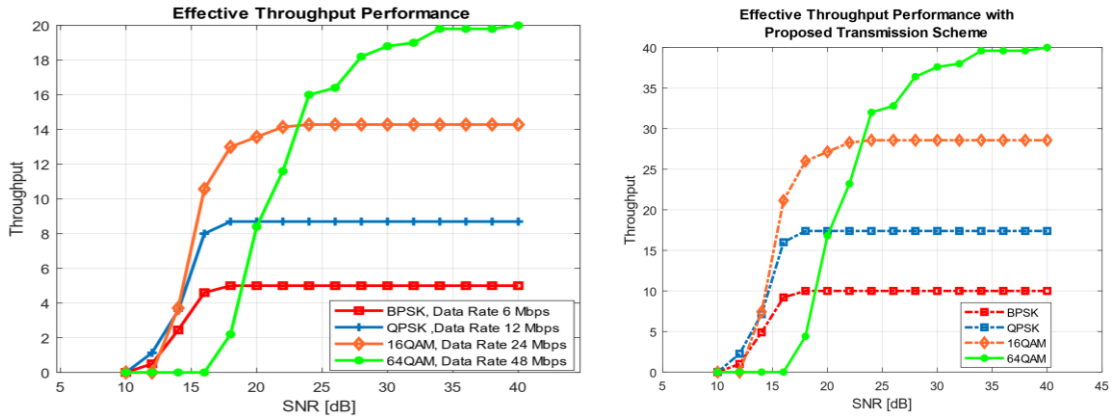

(a) (b)

Figure 11 Effective throughput: (a) the conventional 802.11a system, (b) the proposed transmission scheme in 802.11a system.

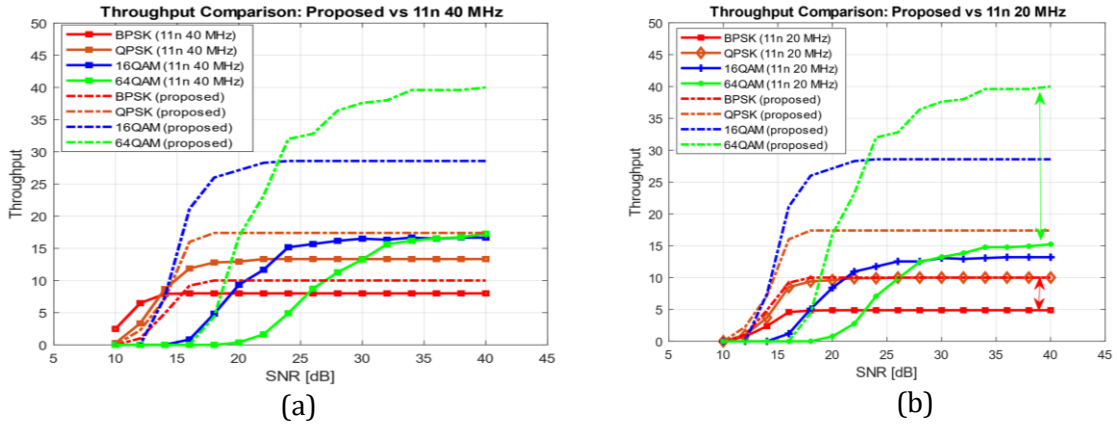

(a) (b)

Figure 12 Throughput performance comparison (a) with 40 MHz BW of 802.11n system, (b) with 20 MHz BW of 802.11n system

Moreover, we perform throughput evaluation by comparing it with the conventional 802.11n transmission with 40 MHz, as the benchmark. As shown in Figure 12, the proposed transmission scheme can improve throughput by 1.2 up to 2.3 times compared to 11n transmission mode at 40 MHz. In addition, the proposed system can achieve throughput

improvement of around 2 times up to 2.67 times, as compared to the conventional 802.11 system with 20 MHz bandwidth. The evaluation results reveal that the proposed scheme can deliver higher throughput by using smaller bandwidth. By using bandwidth efficiently, the proposed transmission scheme can avoid huge device interference when deploying large numbers of devices, as expected in Medical IoT deployment.

3.3. Timing Performance

The timing performance, specifically latency processing is evaluated to assess whether the transmission can satisfy the defined upper layer protocol, in which the maximum latency should be less than inter-frame spacing duration (IFS): $T_{max\,latency} \leq T_{IFS}$. In addition, other conditions affect packet latency such as RF switching as well as channel propagation delay. Hence, the packet transmission time should accommodate all these impacts. The latency processing time requirements of PHY design can be modeled as:

$$T_{max\,latency} = T_{HW_{latency}} + T_{MAC} + T_{channel} \quad (9)$$

In a real deployment, the transmission latency will be affected not only by packet duration but also by processing latency (delay) introduced by hardware processing. Figure 13 shows the measured frame length for both the proposed system and the original transmission. The original design (the upper figure), in each frame, requires 12,800 clocks which correspond to 16 μs duration at a system clock of 80 MHz. On the other hand, the proposed transmission scheme only requires 6,400 clocks, which corresponds to 8 μs frame lengths. In addition, the accuracy performance of each system is almost similar, with the MSE error being around 40 dB on average. From this result, the proposed system can improve the transmission latency by about 50% in the same transmission parameters.

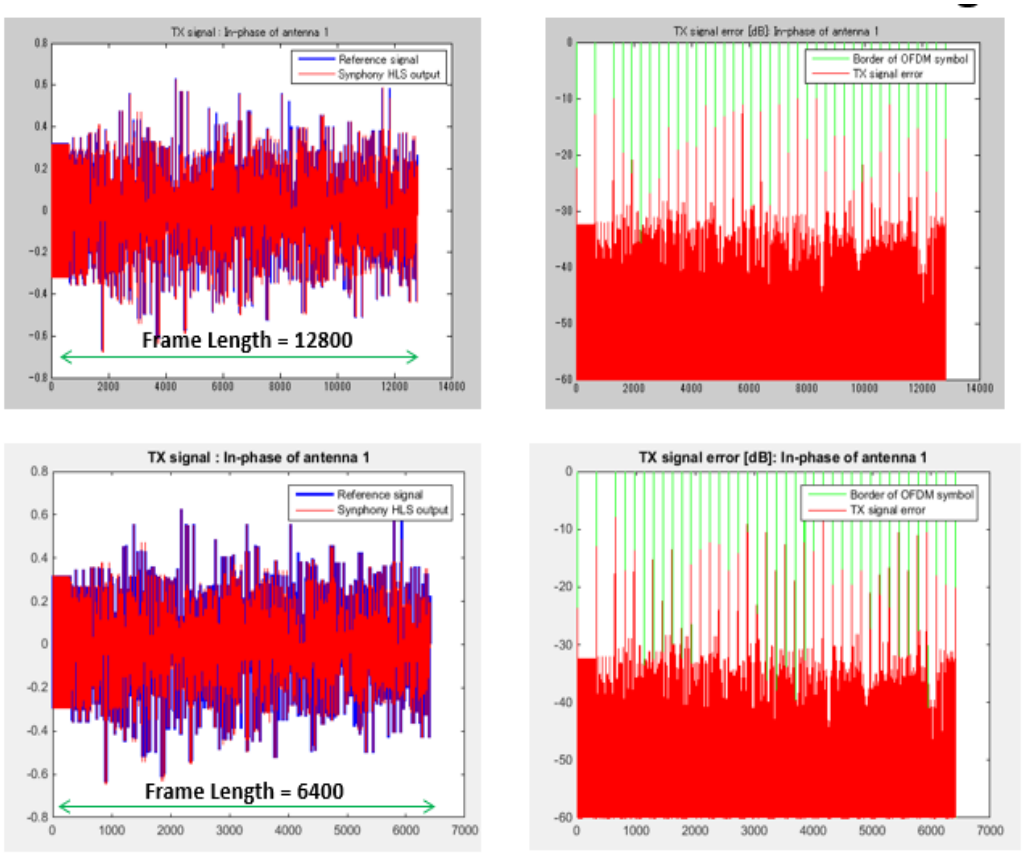

Figure 13 Timing simulation for the transmitted frame of the conventional and proposed scheme

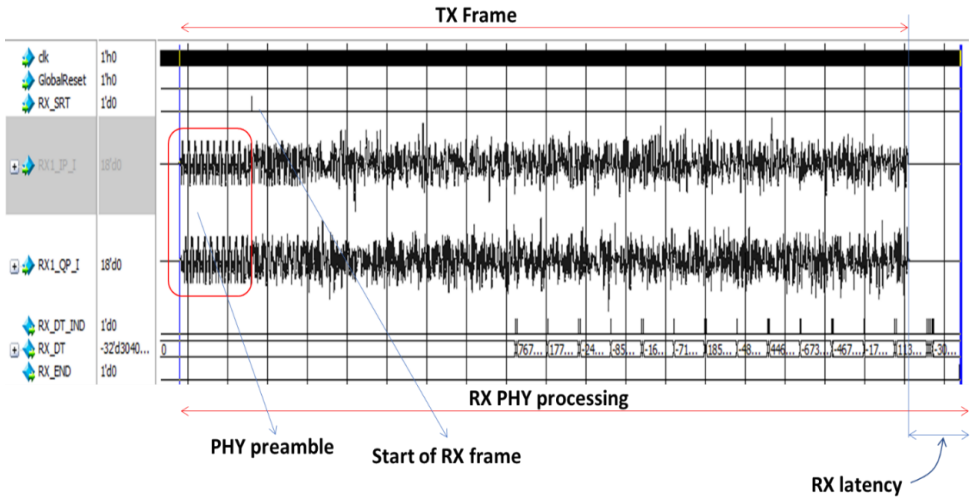

Figure 14 PHY Timing Evaluation

In addition, we also evaluate the processing timing of PHY hardware, as shown in Figure 14. The total timing of the PHY frame is calculated from the start of transmission until all received data is successfully decoded. In this process, the timing latency introduced by all hardware calculations is taken into account. From PHY hardware verification the total RX latency is around 503 clock cycles. This corresponds to 6.29 μs at an operating clock frequency of 80 MHz. This PHY latency is much lower than the latency of the conventional WLAN design as reported by Astri *et al.* (2016), where the latency of PHY is around 12.63 μs. According to verification results, the total latency from PHY is sufficient to catch up with the upper layer protocol in terms of SIFS duration which is 16 μs. Hence, the proposed system can be adopted for low-latency applications.

4. Conclusions

Medical Internet of Things (MIoT) plays an important role to realize smart healthcare systems that offer various scenarios with different performance requirements, in terms of latency and data rate. However, to achieve low latency and high data rate, the existing system wireless mainly employs higher bandwidth, high order modulation, or multi-antenna systems. Such a higher complex system is not preferable for IoT systems. In this work, we have proposed a wireless system with bandwidth-efficient transmission to deliver high throughput and low latency transmission which is important for the deployment in various use cases of healthcare systems. To reduce transmission latency and to utilize lower bandwidth, a cross-layer design method is applied to evaluate and determine optimum transceiver parameters. Specifically, the parameters that affect symbol timing. Furthermore, efficient-bandwidth utilization is obtained by reducing sub-carrier spacing. This implies that transmission in one OFDM symbol can be reduced and can shorten the overall packet. As a result, the design can achieve low-latency transmission. In addition, the corresponding transceiver can be designed with a low-complexity approach. From the experiment, by applying the proposed method, the designed transceiver system can improve the throughput performance by up to 2.6 times compared to the conventional transmission scheme. In addition, the latency performance can be reduced by around 50%, which is possible for achieving low-latency communication with the order of ms end-to-end latency. Therefore, the proposed retransmission scheme could be potentially applied to future MIoT systems that support new use cases, where reliability and low latency performance become the main constraints. The proposed system also offers efficient bandwidth utilization, where the transmission bandwidth is maintained

small to deliver high throughput. The smaller channel bandwidth can minimize channel interference in the deployment of a large number of devices in the same network, which helps to improve reliability performance.

Acknowledgments

This work was partially supported by the ITB Postdoctoral Fellowship Program 2021 (Number 1740/IT1.B07.1/TA.00/2021).

References

Adelabu M.A., Imoize, A.L., Ughegbe, G.U., 2021. Performance Evaluation of Radio Frequency Interference Measurements from Microwave Links in Dense Urban Cities. *Telecom*, Volume 2(4), pp. 328–368

Ahad, A., Tahir, M., Sheikh, M.A., Ahmed, K.I., Mughees, A., Numani, A., 2020. Technologies Trend towards 5G Network for Smart Health-Care Using IoT: A Review. *Sensors*, Volume 20(14), p. 4047

Ahmed, I., Karvonen, H., Kumpuniemi, T., Katz, M., 2020. Wireless Communications for the Hospital of the Future: Requirements, Challenges and Solutions. *International Journal of Wireless Information Networks*, Volume 27, pp. 4–17

Alam, M.M., Malik, H., Khan, M.I., Pardy, T., Kuusik, A., Moullec, Y.L., 2018. A Survey on the Roles of Communication Technologies in IoT-Based Personalized Healthcare Application. *IEEE Access*, Volume 6, pp. 36611–36631

Ali, S., Al-Balushi, T., Nadir, Z., Hussain, O.K., 2018. Improving the Resilience of Wireless Sensor Networks Against Security Threats: A Survey and Open Research Issues. *International Journal of Technology*, Volume 9(4), pp. 828–839

Astri M.K, Lam, D.K., Lanante, L., Nagao, Y., Kurosaki, M., Ochi, H., Areni, I.S., 2016. Design of WLAN Based System for Fast Protocol Factory Automation System. *In:* 22nd Asia-Pacific Conference on Communications (APCC)

Azim, A., 2013. Computational Performances of OFDM Using Different FFT Algorithms. *International Journal of Communications, Network and System Sciences*, Volume 6(7), pp. 346–350

Durisi, G., Koch, T., Popovski, P., 2016. Toward Massive, Ultrareliable, and Low-Latency Wireless Communication with Short Packets. *In:* Proceedings of the IEEE, Volume 104(9), pp. 1711–1726

Erceg, V., Schumacher, L., Kyritsi, P., Molisch, A., Baum, D.S., Gorokhov, A.Y., Oestges, C., Li, Q., Yu, K., Tal, N., Dijkstra, B., Jagannatham, A., Lanzl, C., Rhodes, V. J., Medbo, J., Michelson, D., Webster, M., Jacobsen, E., Cheung, D., Prettie, C., Ho, M., Howard, S., Bjerke, B., Jengx, L., Sampath, H., Catreux, S., Valle, S., Poloni, A., Forenza, A., Heath, R.W., 2004. *TGn Channel Model, Doc.* IEEE802.11-03/940r4. Available online at: https://mentor.ieee.org/802.11/dcn/03/11-03-0940-04-000n-tgnchannelmodels.doc, Accessed date Ooctober 25, 2021

IEEE, 2013. *IEEE Std 802.11ac-2013: IEEE Standard for Information Technology--Telecommunications and Information Exchange Between SystemsLocal and Metropolitan Area Networks-- Specific Requirements--Part 11: Wireless LAN Medium Access Control (MAC) And Physical Layer (PHY) Specifications--Amendment 4: Enhancements For Very High Throughput For Operation In Bands Below 6 Ghz*, IEEE, pp. 1–425

Jagadeeswari, V., Subramaniyaswamy, V., Logesh, R., Vijayakumar, V., 2018. A Study on Medical Internet of Things and Big Data in Personalized Healthcare System. *Health Information Science and Systems,* Volume 6, p. 14

Janjua, M.B., Duranay, A.E., Arslan, H., 2020. Role of Wireless Communication in Healthcare System to Cater Disaster Situations Under 6G Vision. *Frontiers in Communications and Networks*, Volume 1, p. 610879

Skorin-Kapov, L., Matijasevic, 2010. Analysis of QoS Requirements for e-Health Services and Mapping to Evolved Packet System QoS Classes. *International Journal of Telemedicine and Applications,* Volume 2010(4), p. 628086

Luvisotto, M., Pang, Z., Dzung, D., Zhan, M., Jiang, X., 2017. Physical Layer Design of High-Performance Wireless Transmission for Critical Control Applications. *IEEE Transactions on Industrial Informatics*, Volume 13(6), pp. 2844–2854

Marques, G., Pitarma, R., Garcia, N.M., Pombo, N., 2019. Internet of Things Architectures, Technologies, Applications, Challenges, and Future Directions for Enhanced Living Environments and Healthcare Systems: A Review. *Electronics*, Volume 8(10), p. 1081

Ng, J.R., Goh, V.T., Yap, T.T.V., Shuib, M.K., 2019. Adaptive Redundancy-Based Transmission for Wireless Sensor Networks. *International Journal of Technology*, Volume 10(7), pp. 1355–1364

Rukmani, P., Ganesan, R. 2016. Enhanced Low Latency Queuing Algorithm for Real Time Applications in Wireless Networks. *International Journal of Technology*. Volume 7(4), pp. 663–672

Schaich, F., Wild, T., Chen, Y., 2014. Waveform Contenders for 5G - Suitability for Short Packet and Low Latency Transmissions. *In:* IEEE 79th Vehicular Technology Conference (VTC Spring)

Shukla, S., Hassan, M.F., Khan, M.K., Jung, L.T., Awang, A., 2019. An Analytical Model to Minimize the Latency in Healthcare Internet-Of-Things in Fog Computing Environment. *Plos One,* Volume 14(11), p. e0224934